



A bi-material FDM system with reinforced mixing and cooling for uniform material mixing and broad functionality

Li Yang¹ · Henrik Petterson¹ · Jonathan Olofsson² · Philip Palmaer³

Received: 1 July 2024 / Accepted: 5 December 2024
© The Author(s) 2024

Abstract

This work presents a single-nozzle/bi-extrusion FDM technology featuring two material inputs and heating sections connected with a mixing device with a reinforced mixing mechanism. The device ensures uniform mixing of materials, consistent print quality, and functionality, while an air-cooling system allows printing with materials having different solidification temperatures. Trials with six Dryflex TPEs demonstrated precise regulation of material flows, enabling dynamic adjustment of material blends and creation of multiple functionalities in one product. The technology also creates functionally graded materials (FGMs) in transition zones, improving interlayer adhesion and mechanical performance. This advancement enhances production flexibility, efficiency, and product quality, and expands material availability for additive manufacturing.

Keywords Multi-material 3D printing · Functionally graded materials (fgms) · Uniform material mixing · Seamless material transition

1 Introduction

Achieving sustainable industrial and economic development presents a global challenge, necessitating a significant transformation of current production and value chain management practices. Additive manufacturing (AM), a swiftly advancing technology has the capacity to reshape key elements of product design, manufacturing processes, distribution networks, and supply chains [1]. AM offers numerous benefits, including the remarkable ability to create intricate structures, significantly reduce material waste, and enhance cost-effectiveness, particularly for small production runs. Moreover, the application of AM technologies in various industries has expedited product development cycles, enabled personalization and on-demand production, and facilitated the production of complex components previously deemed challenging to manufacture. Industries ranging

from consumer goods and healthcare to automotive and aerospace have already recognized and embraced its potential [2, 3]. Yet, challenges remain that must be addressed to fully unleash the capabilities of AM, including the need for advanced AM technologies, more robust quality control measures, and a wider selection of material options.

Extrusion-based 3D-printing technology commonly known as Fused Deposition Modelling (FDM) or Fused Filament Fabrication (FFF), is a prominent AM technology [4, 5]. Developed by S. Scott Crump in the late 1980s, FDM has seen significant advancements over the last 10 to 15 years, in terms of materials, processes, and applications [6]. FDM has evolved into one of the most popular and extensively used 3D-printing technologies, with applications across diverse industries [7]. It is utilized for tasks ranging from rapid prototyping to the manufacture of end-use parts. The accessibility and adaptability of FDM have significantly contributed to its widespread adoption and ongoing advancements in the field of AM [7].

Commercial FDM systems commonly rely on a single structural material. Nevertheless, there is a discernible trend towards development of multi-material techniques which enable fabrication of intricate and exceptionally functional products with unparalleled complexity [1]. Prajapati et al. demonstrated a concept of light weight closed-cell lattice structures, where the closed-cell lattice structures were 3D

✉ Li Yang
li.yang@ri.se

¹ RISE Bioeconomy, Drottning Kristinas Väg 61,
11428 Stockholm, Sweden

² KFM Maskin I Sverige AB, Floragatan 7,
S-280 40 Skånes Fagerhult, Sweden

³ Hexpol TPE AB, Gamla Örnäsgatan 15, S-662 22 Åmål,
Sweden

printed with thermoplastic polyurethane (TPU) filaments while the close-cell was filled with polyurethane (PU) foam [8]. The multi-material closed-cell foam-filled lattice structures exhibited enhanced mechanical and functional properties such as higher stiffness, energy dissipation, and damping characteristics.

Existing multi-material FDM systems can be categorized into two main groups: those equipped with either a single extruder or multiple extruders [9, 10]. The single extruder system is enhanced either through software modifications enabling filament swapping or through additional hardware like the Mosaic Palette. The multiple extruders system extends the single extruder method by integration of several extruders one per material, side-by-side. RoVa3D is one such system, equipped with five nozzles for five filaments [11].

An object printed with multi-nozzle/multi-feed FDM systems has binary material (interlayer) interfaces. The quality of interlayer adhesion between the material layers is crucial in determining the overall strength of the print [12]. While this may not be an issue for 3D color printing, where identical base materials are used in all color filaments, it is often a concern when printing with dissimilar materials. Lopes and colleagues [13] studied the interlayer adhesion between PLA and two immiscible polymers, TPU and PET. Zebra crossing-like tensile test specimens were printed with dual-material/dual-printing heads. The tensile strengths of the hybrid material test specimens were 6.5 MPa for PLA-TPU and 12.2 MPa for PLA-PET combinations, while the tensile strengths of the pure materials were 64.0 MPa for PLA, 30.3 MPa for TPU, and 47.7 MPa for PET. The dramatic decreases in tensile strength values for the hybrid material test specimens were due to poor adhesion at the interfaces between the immiscible materials. A similar study was conducted by Baca et al. [14].

In addition to multi-nozzle/multi-feed FDM systems, single nozzle/multi-feed FDM printers using filament materials as inputs are also documented in the literature. Khondoker et al. presented a bi-extruder FDM system capable of printing two thermoplastic filaments through a single output nozzle using a static inter-mixer for the input materials [15]. In this configuration, two material streams were merged within the converging section, forming a mechanical interlock, and were subsequently deposited onto the previously printed layer through the single-nozzle orifice. While the mechanical interlock somewhat improved adhesion between the input materials, the inter-mixer failed to blend the materials homogeneously, as observed from the microscope images of cross-sections of the extrudates [15]. In addition, several open-source FDM systems with similar characteristics from the hobbyist community have emerged [9]. These systems have mainly been used to build 3D parts in color using color filaments made of the same base material, like PLA [15].

The necessity to convert materials into filaments limits the material availability and, in turn, the applicability of these systems in broad industrial application.

Functionally graded materials (FGMs) are a novel type of engineering material whose properties gradually change with position [16, 17]. AM has great potential in functionally gradient additive manufacturing (FGAM), enabling a radical shift from contour modelling to performance modelling [18]. Methods such as material jetting, laser metal deposition, and powder metallurgy have been instrumental in fabricating intricate FGM structures with enhanced functionalities [16]. For example, Mora and colleagues [19] experimented with 3D-printed architected lattice structures using a material jetting process. They utilized multiple nozzles to deposit droplets of various photopolymers, which were subsequently cured by UV light. Reichardt and his team provided an exhaustive overview of advancements in AM concerning metal-based FGMs, encompassing the fabrication of FGMs using an array of stainless steel, nickel, titanium, and copper alloys [20].

Several works on FGAM using FDM technology have been reported in recent reviews [16, 18]. Among these, Li et al. printed FDM models using two separate extruders: one for acrylonitrile butadiene styrene (ABS) filament as the model material and another for wax as the support material [21]. By switching the extruders at will, they fabricated structures with different mechanical properties. Multi-material FDM systems equipped with a converging and static mixing device that combines material streams into a single output nozzle represent the state of the art in FDM technology [14, 15]. This technology allows the fabrication of FDM models with variable material mixing ratios. Very recently, researchers have developed a two-step process for multi-material FDM 3D printing, called blended FDM or b-FDM, to create parts with specific gradient material properties [22]. A dual-extruder system is used in the first step to create an intermediate filament, by depositing base materials layer by layer. The 3D printed filament, having programmed material blends in different sections, is manually fed to one of the extruders of the dual-extruding system to create the final print with variable material compositions & properties within the same printed part.

Existing multi-material FDM methods, whether multi nozzle or single nozzle, have limitations. The multi-nozzle FDM method creates discontinuities in the structure when switching from one material (nozzle) to another. This material switching not only takes time but also deteriorates mechanical performance, as the discontinuity often becomes the weakest link in the structure. The multi-feed, single-nozzle FDM systems equipped with a static mixer may not achieve homogeneous material mixing, as observed in previously reported studies [15, 23]. In addition, these systems cannot process materials other

than filaments. The need for filament conversion increases material costs and limits material availability and flexibility for industrial applications. Moreover, there are challenges in building parts with materials that have significantly different thermal properties, such as melting, glass transition, and solidification temperatures. Reinforced cooling to maintain the shape of the freshly printed layer can be crucial, as will be discussed later.

In this work, we introduce a new bi-extruding system that can cope with polymeric granulates. With the inbuilt reinforced mixing and cooling mechanisms, the system facilitates homogeneous material mixing and dynamic & seamless material transitions. This allows one to create intricate structures and broad functionalities with a few material combinations. Materials compatibility was only

explored in short term in the present work, no long term durability was extensively dealt with.

2 Materials and methods

2.1 Working principle of the multi-polymer FDM printer

The multi-material FDM printer is equipped with two extruders but only one output nozzle. The working principle and structural details are depicted in Fig. 1a, where two material streams converge and mix in the mixing zone, and the blended material is ejected from the output nozzle. Figure 1b shows the inner structure of the mixing device,

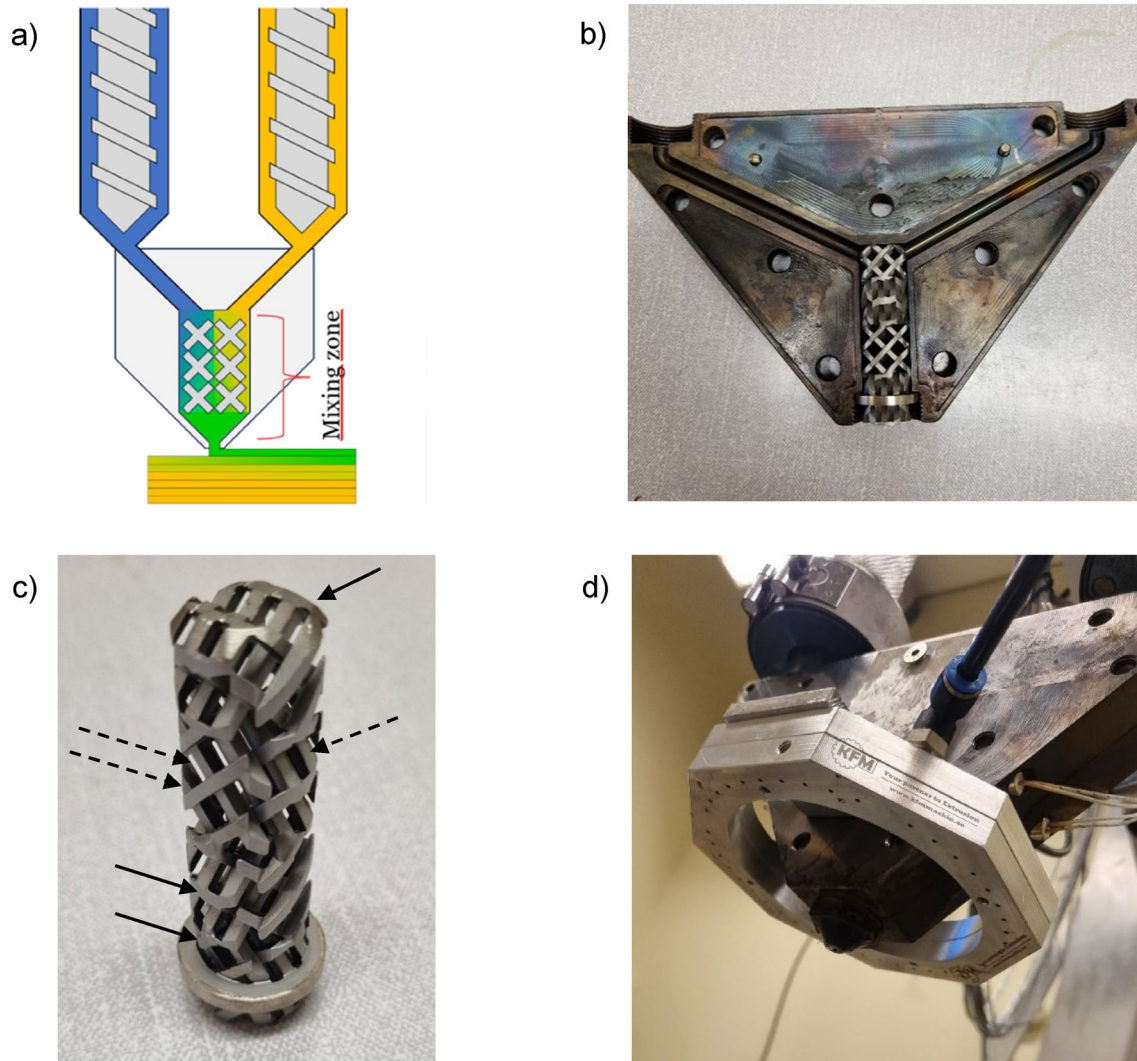


Fig. 1 The multi-material FDM printing system. **a** Illustration of the working principle, **b** the converging & mixing device with the insert for reinforced mixing, **c** a close-up of the insert for reinforced mixing,

d a close-up view of the output nozzle of 2 mm, surrounded by the air-cooling device

which includes a reinforced mixing mechanism inserted into the mixing zone. The insert facilitates material mixing within a short mixing length. Figure 1c is a close-up of the reinforced mixing insert, which consists of multiple interconnected comb-like structures in two orientations that are perpendicular to each other. For an easier appreciation, solid and dashed arrows are added, pointing to some sloping comb-like structures. These structures force the material streams to merge and split multiple times, facilitating material mixing, before being jetted out. Finally, Fig. 1d offers a close-up view of the output nozzle (no shown in Fig. 1b), which connects to the end of the mixing insert. By employing nozzles with different opening sizes, filaments of different diameters can be ejected.

The heating temperatures and material flows in the respective extruding channels can be separately regulated through software. This allows the relative portions of the materials to be dynamically regulated at will in the printing (production) run, enabling continuous and seamless transitions in material composition and functionality. To accommodate materials with significantly different solidification temperatures or softness, an air-cooling system is incorporated around the orifice, as shown in Fig. 1d. The cooling air regulates and accelerates the solidification of the freshly deposited layer, maintaining its shape and enabling uninterrupted 3D printing of various material compositions.

2.2 Materials

The materials tested in this work included six Dryflex TPEs (thermoplastic elastomers) provided by Hexpol TPE AB, comprising three soft and three hard variants. These TPEs span a broad range of hardness and rheological characteristics as indicated in Table 1. The softest TPE has a hardness of 35 Shore A, while the hardest has a hardness of 70 Shore D. The choice of materials was motivated by the need to achieve a wide of range of mechanical properties

Table 1 Information of the Dryflex TPEs materials. #547 was made with addition of glass fiber

Materials Product No	Hardness		MFR [g/10 min]	Comment
	Shore A	Shore D		
#548	35		28 (190 °C/2.16 kg)	
#550	45		11 (190 °C/2.16 kg)	
#309	48		13,4 (190 °C/5.0 kg)	
#310		67	17,8 (190 °C/5.0 kg)	
#546		70	40 (190 °C/5.0 kg)	
#547		70	15 (190 °C/5.0 kg)	With glass fiber

important for the intended demonstrative applications, such as prostheses and orthoses. In the table, the numbers in the fourth column represent the mass flow rate (MFR) of the materials, with the numbers in parenthesis indicating the testing temperature and the pressure applied during the MFR measurements. Regardless of the hardness, the MFR varies significantly between materials. For example, material #547 has essentially the same hardness (70 Shore D) as material #546, but its MFR is only about one-third of that of material #546, likely due to the inclusion of glass fibre in material #547.

In addition to their diverse mechanical properties, the TPEs also exhibit a broad range of optical properties, from highly transparent to opaque. Figure 2 shows the appearances of the six TPEs used in this work. Visual inspections revealed that #309 is the most transparent, followed by #310, and #550. Materials #546 and #548 have lower transparency, while the glass fiber containing material #547 is opaque.

2.3 Mechanical tests of 3D printed samples and demonstrator

Two types of printed samples were created for mechanical test according to ISO 3167 [17]. Various combinations of the materials listed in Table 1 were utilized to produce these samples, incorporating different ratios of material mixing. For simplicity, without losing generality, material blends in five distinct mixing ratios (0:100, 25:75, 50:50, 75:25, 100:0) in v% were reported.

The test specimens were fabricated with line patterns in two orientations relative to the mechanical testing direction,

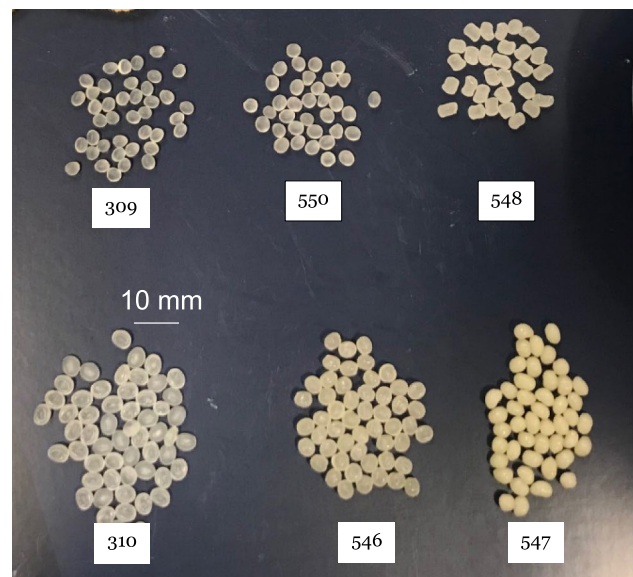


Fig. 2 Images of the Dryflex grade TPEs, three soft TPEs (top row), three hard TPEs (bottom)

as indicated by the double-arranged lines in Fig. 3. In sample A, the printed line patterns align parallel to the mechanical testing direction. Conversely, in sample B, the line patterns run perpendicularly to the mechanical testing direction (Z). Hence, letter Z is added to the name of the type B samples.

Two additional test specimens were created to demonstrate the difference in interlayer adhesion between the test pieces built with the multi-nozzle method and those built with the present method. In Fig. 4, samples in the hexagonal column (left) and the square column (right) were created with the same pair of materials, e.g. soft TPE (#550) and the hard TPE (#546). The data labels in the figure indicate the relative volume percentages of the soft TPE (#550) in the respective sections. The hexagonal column has binary interfaces between adjacent sections, similar to prints with multiple output nozzle method, as there was a purge process before switching to a new material ratio. In contrast, the printing process of the square column was uninterrupted when switching to a new material ratio, resulting in a seamless material transition. The

standard test specimens were then derived from the hexagonal and square columns, respectively, by laser cutting. Detail discussions on the impacts of the material transition interfaces will be given in Sect. 3.

Printing an object with sections of multiple material compositions is achieved by creating virtual tools in the printer's hardware. These tools operate consecutively, with the ending position of the current tool being the same as the starting position of the next. Each virtual tool has two extruder outputs, A and B, corresponding to two material inputs to the mixing device, whose sum equals unity.

For example, to print an object consisting of two sections with different mixing ratios of materials #309 and #546, such as 75% (#309) & 25% (#546) and 30% (#309) & 70% (#546) in volume, two virtual tools are needed. In tool #1, the extruder outputs are 0.75 for extruder A (#309) and 0.25 for extruder B (#546). In tool #2, the corresponding extruder outputs are: 0.30 for extruder A (#309) and 0.70 for extruder B (#546).

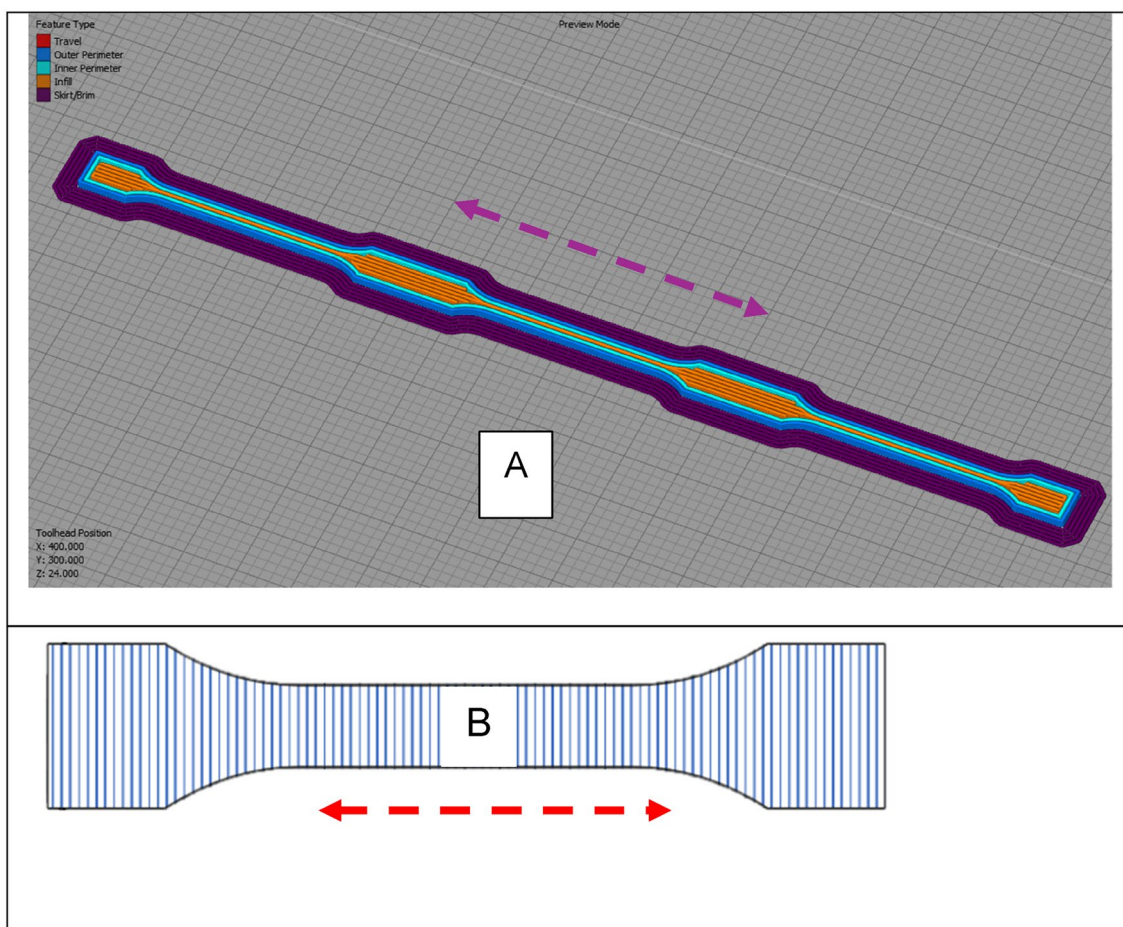
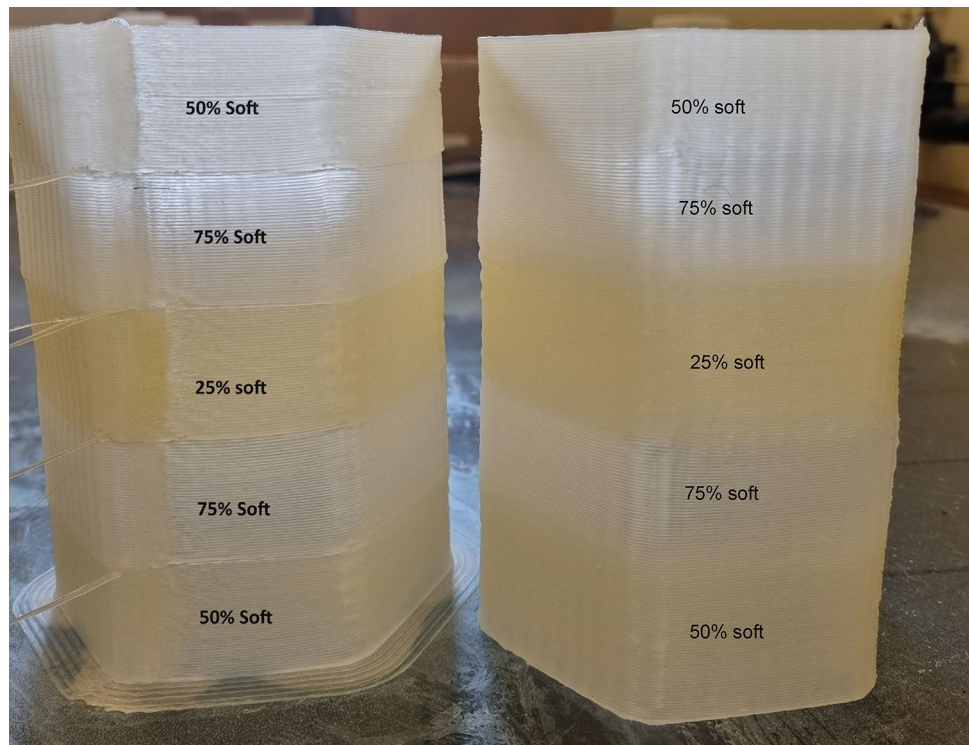


Fig. 3 The layouts of mechanical test specimens with their building directions along or cross the mechanical testing direction indicated by the double-arranged lines

Fig. 4 Images of the hexagonal column (left) and the square column (right) printed with mixtures of two TPEs, the soft TPE (#550) and the hard TPE (#546), in five relative mixing ratios. The data labels indicated the relative volume percentages of the soft TPE. The hexagonal column had binary interfaces between the adjacent sections while the square column had functionally graded material zones



Since all the virtual tools correspond to the same physical printer hardware, there is no interruption in the printing process during the transition. Moreover, when transiting from tool #1 to tool #2, the material compositions change gradually, creating an FGM zone rather than binary material transition (interface), which benefits layer-to-layer adhesion. This approach allows for the realization of any number of virtual tools with different mixing ratios.

A universal testing machine, MTS 400/M, equipped with pneumatic grips and a 2 kN load cell, was used for tensile testing. The tests were conducted at a rate of 50 mm/min. The results are presented in next session.

3 Results and discussions

3.1 Mechanical properties of different material blends

The mechanical testing data of the standard test pieces, directly 3D printed or type A, is collectively presented in Table 2. The data correspond to four pairs of the TPE materials, one soft and one hard in each pair. The relative portions of the materials in each pair varied in four equally spaced nominal intervals, 100% to 25% for the soft material or 0 to 75% for the hard one.

In the table, data in column 4 are the peak stress values at which the test samples either broke or reached the

maxima of their stress curves. The strain at break of the test samples is given in column 5, where the data in red denote the never broken sample when its tensile strain exceeded 550%. In addition to the peak stress values, Young's modulus (column 6), yield stress (column 7), and yield strain (column 8) indicating the range of elastic deformation have also been given in the table.

Plots in Fig. 5 were plotted from the mechanical data shown in Table 2. The mechanical properties of the material blends vary nonlinearly with their relative material compositions. For one pair of the materials, its peak stress value is dominated by that of the hard material. Hence, by varying the relative portions of the materials, one can obtain material blends whose properties (functionalities) span the whole range in between the properties offered by the pair of materials.

The modulus and the yield-stress values follow similar trend. On the contrary, the yield strain decreased non-linearly with the increasing percentage of the hard material. Among the four plots in each figure, three of the plots correspond to the material blends having the same hard material (#547) but different soft materials, #309, #548, and #550, respectively. It is obvious that the soft materials also had strong impacts on the mechanical properties of the material blends, even at high percentage of hard material. This is positive in an application perspective as it extends the range of the mechanical properties offered by the material mixing.

Table 2 Mechanical properties of the tensile test samples (type A) printed by combining one soft with one hard material of the Dryflex grade. The measured values are from three or more print samples

Material blends		Peak Stress	Strain at	Modulus	Yield stress	Yield strain
Soft (%)	Hard (%)	(MPa)	break (%)	(MPa)	(MPa)	(%)
100	0	2,06 (0,09)	> 550	2,7 (0,1)	1,07 (0,06)	150,9 (5,8)
Soft: #309	75	3,26 (0,38)	> 550	11,6 (5,4)	1,83 (0,28)	104,9 (25,6)
Hard: #310	50	8,77 (0,67)	51 (11)	204,0 (23,5)	7,93 (0,61)	12,6 (1,0)
	25	19,56 (0,18)	25 (8)	574,3 (28,2)	17,44 (0,25)	8,2 (0,4)
100	0	2,06 (0,09)	> 550	2,7 (0,1)	1,07 (0,06)	150,9 (5,8)
Soft: 309	75	4,05 (0,07)	> 550	28,0 (0,1)	2,73 (0,05)	68,5 (0,6)
Hard: #547	50	11,43 (0,47)	16 (2)	421,8 (24,7)	10,03 (0,39)	6,3 (0,4)
	25	32,57 (2,10)	7 (1)	1301,2 (92,9)	25,78 (7,61)	3,6 (1,3)
100	0	1,70 (0,00)	> 550	1,5 (0,2)		
Soft: #550	75	4,60 (0,17)	103 (8)	95,4 (4,2)	4,08 (0,19)	17,6 (0,8)
Hard: #547	50	27,25 (0,35)	8 (0)	1038,8 (45,4)	24,42 (0,31)	4,9 (0,1)
	25	40,30 (0,00)	6 (1)	1370,5 (52,6)	36,46 (0,57)	4,4 (0,6)
100	0	2,25 (0,07)	> 550	2,9 (0,0)	1,28 (0,09)	197,4 (25,6)
Soft: #548	75	4,70 (0,14)	503 (48)	65,8 (2,9)	3,99 (0,01)	43,3 (1,6)
Hard: #547	50	21,00 (2,16)	7 (2)	913,1 (181,1)	18,89 (1,32)	4,5 (0,8)
	25	40,20 (1,70)	5 (1)	1530,9 (68,5)	37,94 (1,01)	4,0 (0,8)

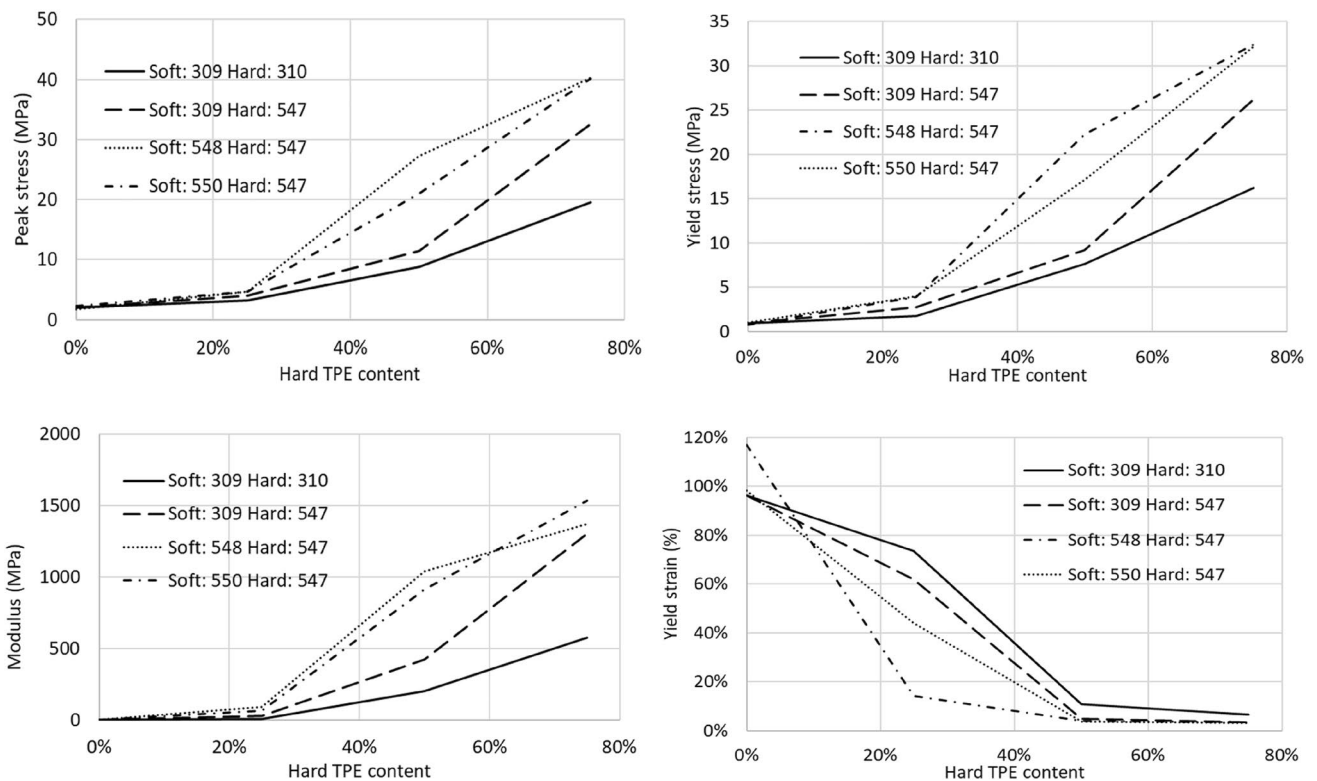


Fig. 5 Mechanical properties of the directly 3D printed dumb-bell pieces (type A) created with different pairs of the materials (one hard and one soft). The x-axis is the relative portion of the hard material

3.2 Influence of building direction on the mechanical properties

Figure 6 illustrates measurements of type B samples. The

samples were made of one soft TPE (#550) and two hard TPES, #546 and #547. The relative material ratios of the soft to the hard are 100:0, 75:25, 50:50, 25:75, and 0:100, respectively. As precedingly stated, the type B sample has its

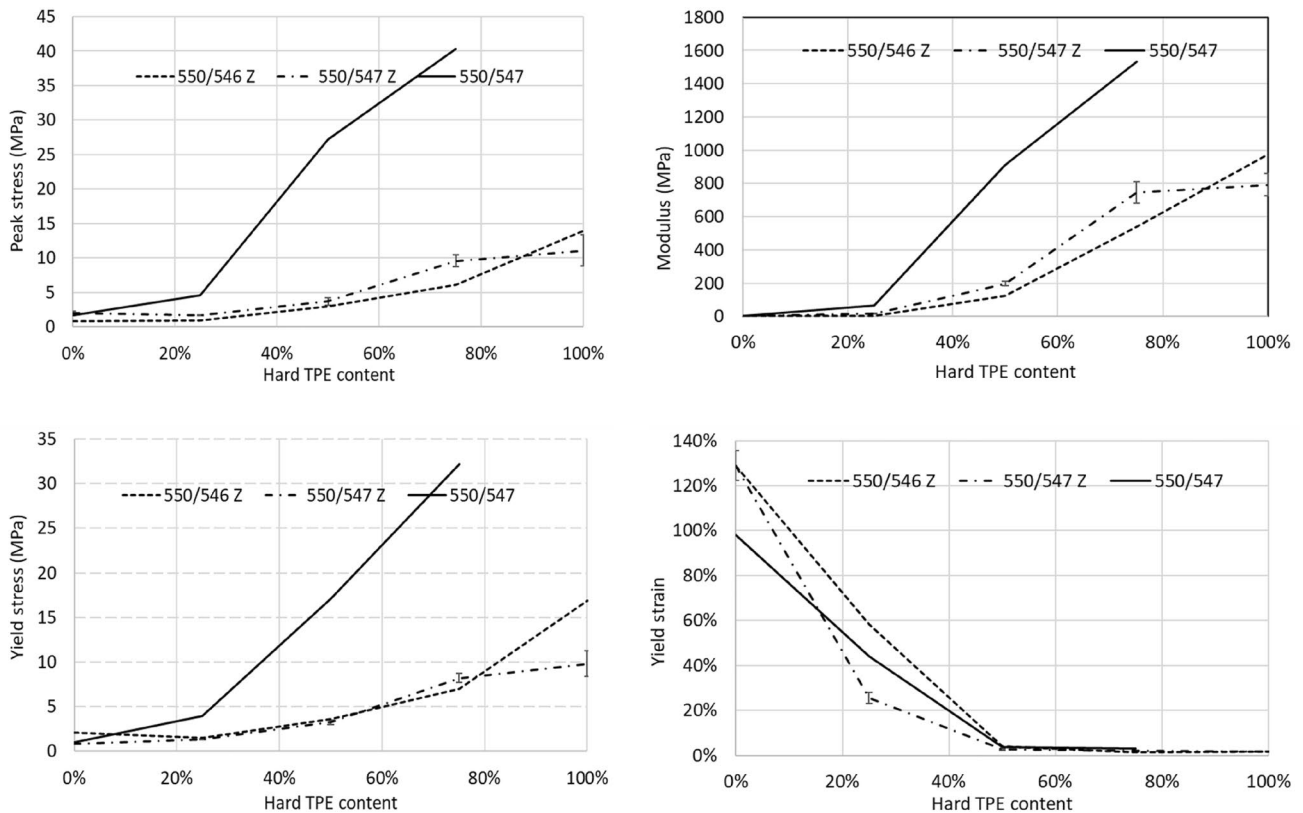


Fig. 6 Mechanical properties of the dumbbell of type B having different material combinations (one hard and one soft)

building direction perpendicular to the direction for mechanical testing, hence the letter Z has been added in the legend.

When comparing with the data of samples made of the same material pair but with different building directions (e.g., 550/547 Z shown in Fig. 6 compared to 550/547 shown in Fig. 5), it is evident that at low content of the hard TPE (< 25%), their stress values differ only marginally. However, the differences grow rapidly with increasing content of the hard TPE. For example, the peak stress values of the type A samples are about 20 MPa at 50% and 40 MPa at 75% of the hard TPE contents while their corresponding values of type B shown in Fig. 6 are about 6 MPa and 11 MPa, respectively.

The reason why the type B samples exhibited lower mechanical properties compared to those of type A can probably be attributed to, at least, three origins as suggested by Majko et al. [24], namely, cool joints or interfaces between already deposited material and the just extruded filament, smaller contact area of two adjacent filaments than the thickness of the printing layer, and the alignment of glass fibers along the printing direction, having essentially no contribution to the layer-to-layer strength. Thus, the mechanical values of type B mainly reflect the layer-layer adhesion of the TPE material blends. Consequently, a high dosage of glass fiber may even lead to deteriorated layer-to-layer bonding strength, as observed below.

The measurement of the material blends of 550/546Z is also shown in Fig. 6, where the TPE #546 has the same Shore D hardness as TPE #547 as shown in Table 1. Their mechanical behaviors of the material blends, 550/546Z and 550/547Z, exhibit similar evolution with respect to the hard material contents up to 75% of the hard TPEs beyond which their relative magnitudes reverse in position. This may imply that addition of glass fibers results in lower layer-layer adhesion (binding strength) compared to that of its counterpart without glass-fiber addition.

3.3 Adhesion and material transition interfaces

Figure 7 shows the standard test specimens derived from the hexagonal and square columns shown in Fig. 4, both before and after the tensile tests. The test specimens consist of five sections, with the percentages of soft TPE in each section indicated by the data labels. The break point of each test specimen represents the mechanically weakest position. Since the nominal material compositions of each test specimen are symmetric about its middle section, the mechanical performance of the test specimens should also be considered symmetric.

The images on the left of Fig. 7 show the test specimens, before and after the tensile test, with binary

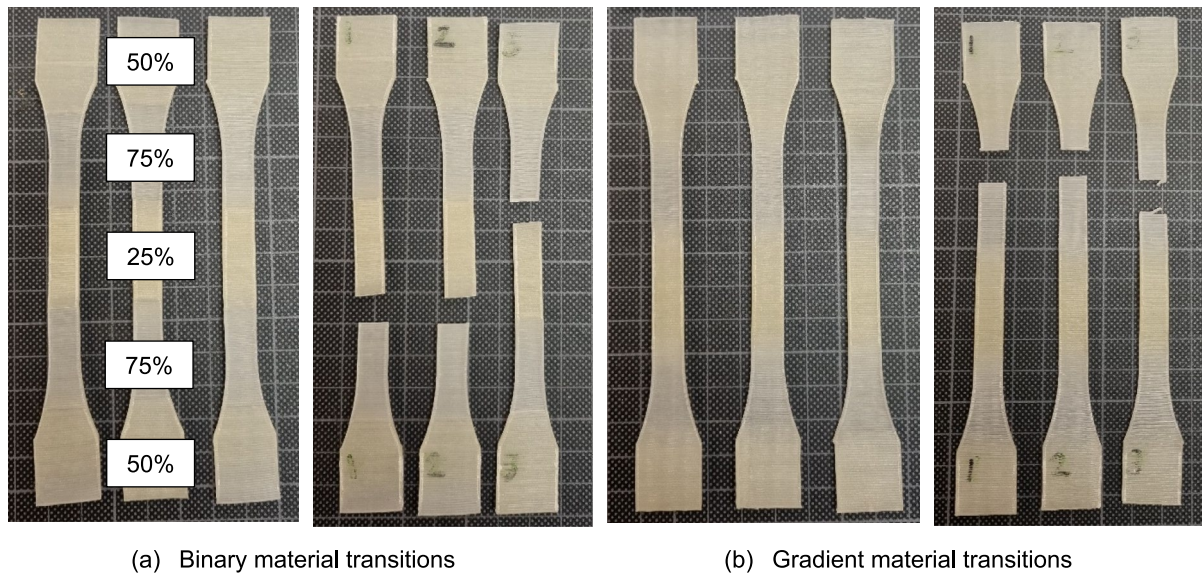


Fig. 7 Tensile test specimens consisting of multiple sections made of different material mixing ratios, where the data labels show the percentages of the soft TPE. The test specimens have (a) sharp or binary material transitions and (b) gradient material transitions

material-transition interfaces —typical when using multi-nozzle FDM systems. The images show that the mechanical failures occurred precisely at the interfaces either above or below the middle section, or at the interfaces between the section with 75% and that with 25% of soft TPE. This indicates weaker interlayer adhesion at these interfaces.

Conversely, for the test specimens with gradual material transition zones created with the present method, shown on the right half of Fig. 7, their positions of mechanical failures are in the middle of the sections consisting of 75% of soft TPE rather than at any of their interfaces. This suggests that the introduction of transition zones has indeed improved interlayer adhesion at the interfaces, thereby enhancing the overall mechanical strength of the printed part.

Figure 8 details the mechanical tests, where the dark grey bars represent peak stress values, and the light grey bars represent strain at break. The test specimens with gradual transition zones have an average peak stress of 1.6 MPa that is comparable to that of the 550/546 Z specimen shown in the top left image of Fig. 6, where the peak stress of the specimen, having 75% of #550 and 25% of #546, is about 1.7 MPa. This peak stress value of the test specimens with gradual transition zones is about 30% higher than that with binary interfaces. This difference should be considered as significant because the adjacent sections were made of the same materials, #550 and #546, differing only in their mixing ratios. In case of interfaces between dissimilar materials, for instance PLA-TPU or PLA-PET as demonstrated by Lopes [13], their difference can be much greater.

The difference is more pronounced in the strain at break. In the case of binary transition (light grey bar on

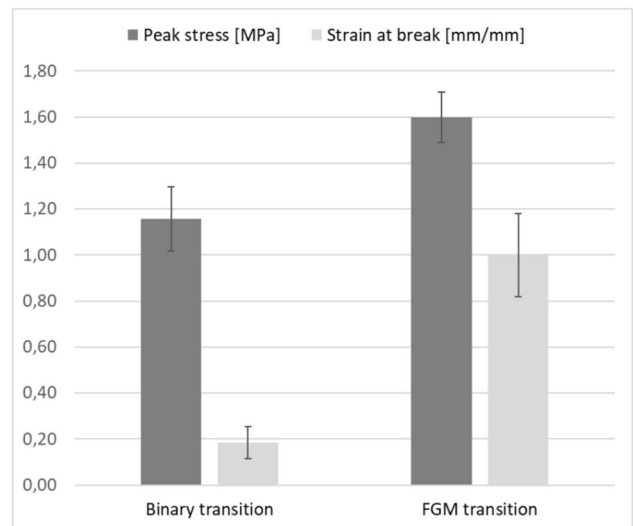


Fig. 8 Comparisons of the average peak tensile stress and the strain at break of the test specimens shown in Fig. 7, having either binary (left) or FGMs (right) transitions

the left), the strain at break is low or less than 20% since the break occurred at the interfaces due to delamination. While the strain at break is five times as much in the case of gradual transition (light grey bar on the right) or with 100% strain at break. This is strong evidence saying that the break occurred in the middle of the section with 75% soft TPE, which is the weakest section among all sections of the entire test specimen.

3.4 Uniformity of material mixing

Figure 9 shows the image of the demonstrator, printed with two polymeric granules—#309 with red pigment added and #310 without. During printing, the relative portion of the red material decreased gradually with height, while the colorless material increased, resulting in continuous shift in color shading. It is evident that the printed demonstrator exhibits smooth transitions with height in both geometry and color.

To examine the efficiency of the reinforced mixing device, prints with mixtures of colored polymeric streams were made. Two color pigments, one red and one blue, were added to the respective material inputs of the FDM printer, one color per granulate input. The granulates melted and mixed with the pigments in their respective extruding



Fig. 9 3D shaped demonstrator created by mixing two polymer granulates, #309 with red additive and #310 color-less. The relative portion of the red decreases gradually from the bottom to the top

sections. Then, the colored polymeric streams met and mixed in the mixing section.

Figure 10 shows the reflective cross-section images of two prints, captured with a stereo microscope, Nikon SMZ-U. The magnification was 4x, giving an image of 5.2 mm in length. The prints had two different mixing ratios, 25% red & 75% blue and 50% red & 50% blue, respectively.

The images clearly show the contours of the printed patterns layer-by-layer with good joint (interlayer adhesion) between the layers. The mixing of the colored streams within both prints was largely uniform across the whole cross section area, except for some reddish regions around the perimeters of the melt filaments.

4 Discussions

The existing multi-material FDM techniques, with either a single hot end or multiple hot ends [9], have limitations or drawbacks. In the single hot end method, multiple filament segments are spliced into a single threaded filament and printed, known as programmable filament [25]. The printer works at the same temperature throughout the printing process regardless the sliced filaments. Hence, this technique has mainly been used in 3D color printing, where the filaments are made of the same base material and different color additives. For the multiple hot end methods, the incorporation of multiple extruders and output nozzles, one for each material, increases the weight of the 3D-printing system, adversely affecting its performance in terms of mobility, stability, precision, repeatability, and printing speed. It is thus impractical to operate with so many extruders fed with an equal number of premixed filaments that span the whole spectrum of the mechanical properties as demonstrated in Fig. 5. In addition, this setup introduces complexity to the motion system and calibration, requiring adjustments to ensure the proper alignment of the print heads. Moreover, every switch

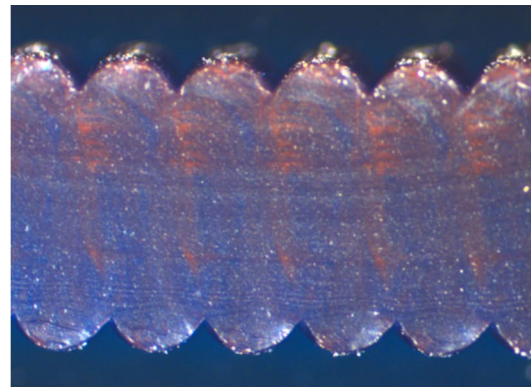
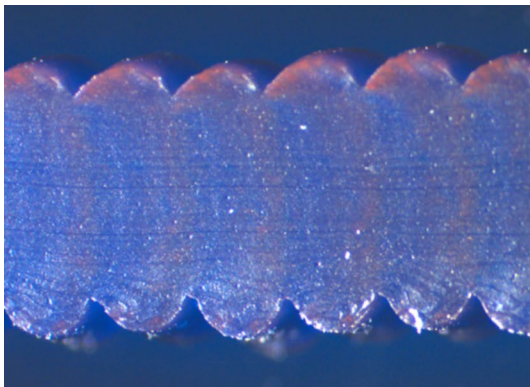


Fig. 10 Microscopic cross section images of prints with two colored polymeric granulates in different mixing ratios, left: 25% red & 75% blue; right: 50% red & 50% blue

between materials (extruders/nozzles) introduces a discontinuity feature, often resulting in weaker mechanical performance of the 3D printed part. Furthermore, these limitations make the multiple hot end methods less appealing compared to the proposed approach that enables dynamically adjustable material compositions at will.

There are two major causes that negatively impact interlayer adhesion and the overall mechanical strength of an FDM built object with multiple materials: poor adhesion between layers of dissimilar materials with binary transitions, which is particularly severe between chemically dissimilar materials such as PLA / TPU or PLA / PET [13]; and discontinuity in the built structure, when switching from one material to another. The proposed method removes these weaknesses and limitations. First, with materials mixing at will, binary material transition interfaces can be avoided by printing one or several gradient layers (of different material mixing ratios or FGMs) in the transition zone. This strengthens interlayer adhesion and the overall mechanical strengths of the 3D printed parts, even with chemically dissimilar materials. Thus, the proposed method also extends material availability for the multi-material FDM process. Second, the printing process continues independently of transition in material compositions. In other words, the material transition occurs seamlessly. Third, different parameters in heating (temperatures) and cooling can be applied for optimal printing performances, enabling broad material availability.

Uniform mixing of materials is essential for mechanical performance of 3D printed parts. The reinforced mixing mechanism introduced in this work represents the major advance in multi-material FDM technology that ensures uniform material mixing and functionality. Yet, the materials compatibility was explored in limited manner, more extensive investigations on long term durability may be needed.

Reinforced cooling measures have also been important when printing / building with materials having significantly different melting and solidification temperatures and/or softness. For example, when printing with the pair of materials #309 and #546, reinforced cooling was needed to maintain the freshly printed layer in shape when the relative composition of the soft TPE (#309) was higher than 50 v%. In this work, the flow rate of cooling air was manually regulated. Further developments in software that can precisely and dynamically regulate the material flows and cooling air's flow will eventually release the full potential of the technology.

The proposed multi-material FDM technology brings forth several distinct advantages. (1) Improved material availability: finding materials suitable for different AM processes has been challenging. Being able to mix materials at will in situ of 3D printing adds an extra dimension to material availability, as a diverse range of functionalities can be achieved by mixing two or a few materials available

for 3D printing. For instance, by mixing one hard (rigid) material with one soft (flexible) material in different relative portions, various levels of hardness and softness can be achieved between those of the individual materials. (2) Enhanced production flexibility and potential for automation: The 3D printer, utilizing the same material inputs, can produce parts with different final properties or functionalities without production stop for hardware reconfiguration or material changes. (3) Increased production efficiency: Through software-controlled adjustment of material flows during printing, the printer can seamlessly create intricate functionalities within a single product and production run. This integration of different functional parts (separately produced with conventional technologies) into one reduces the time and labor for assembling. (4) Enhanced mechanical performance: an uninterrupted printing process and seamless material transition result in FGMs that greatly improve interlayer adhesions between different materials sections and the overall mechanical performance of printed structures. (5) Reduced material management: being able to create a diverse range of functionalities using only a few materials can significantly reduce the number of materials needed for various industrial applications.

5 Conclusions

This study presents a new development of multi-material FDM print technology. It features dual material inputs and extruders connected to a mixing device, which includes a reinforced mixing mechanism as an insert. The mixing device facilitates uniform mixing of two material streams, ensuring consistency in print quality and functionality, while the air-cooling system makes it possible to print with materials having significantly different solidification temperatures and to maintain the freshly laid material layers in shape.

3D-printing trials with six Dryflex TPEs, three soft and three hard TPEs, demonstrated that this technology allows for precise regulation of material flows in the extruders, enabling dynamic adjustment of the relative portions of the material blend and the creation of multiple functionalities in one product and one production run. This technology also enabled achieving a diverse range of mechanical functionalities with only two materials. In addition, by dynamically regulating the material flows through software during printing, the printer seamlessly produced multiple functional zones within a single product and in one production run. Furthermore, the technique created functionally graded materials (FGMs) in the transition zone when switching from one material composition to another. The FGM structure eliminates concerns about poor interlayer adhesion between dissimilar materials and greatly improves the overall mechanical performance of the 3D printed parts. The technology

showcased significant potential for improved production flexibility, efficiency, and product quality. Moreover, being capable of adjusting material blends at will through software in situ during 3D printing introduces an extra dimension to material availability, which has so far been a limiting factor for the industrial adoption of additive manufacturing, as a diverse range of functionalities can be achieved by mixing two or a few materials available for 3D printing.

Funding Open access funding provided by RISE Research Institutes of Sweden. This work has been funded by BioInnovation, a Strategic Innovation Program and a joint effort by Vinnova, Formas and Energimyndigheten [grant number 2021–03711]. The authors have no relevant financial or non-financial interests to disclose.

Data availability The data that support the findings of this study are available on request from the corresponding author.

Open Access This article is licensed under a Creative Commons Attribution 4.0 International License, which permits use, sharing, adaptation, distribution and reproduction in any medium or format, as long as you give appropriate credit to the original author(s) and the source, provide a link to the Creative Commons licence, and indicate if changes were made. The images or other third party material in this article are included in the article's Creative Commons licence, unless indicated otherwise in a credit line to the material. If material is not included in the article's Creative Commons licence and your intended use is not permitted by statutory regulation or exceeds the permitted use, you will need to obtain permission directly from the copyright holder. To view a copy of this licence, visit <http://creativecommons.org/licenses/by/4.0/>.

References

- Kanishka K, Acherjee B (2023) Revolutionizing manufacturing: A comprehensive overview of additive manufacturing processes, materials, developments, and challenges. *J Manuf Proc* 107:574–619
- Alami A, Olabi A, Alashkar A, Alasad S, Aljaghoub H, Rezk H, Abdelkareem M (2023) Additive manufacturing in the aerospace and automotive industries: Recent trends and role in achieving sustainable development goals. *Ain Shams Eng J* 14:102516
- Stenvall E, Flodberg G, Pettersson H, Hellberg K, Hermansson L, Wallin M, Yang L (2020) Additive manufacturing of prostheses using forest-based composites. *Bioeng*. <https://doi.org/10.3390/bioengineering7030103>
- Goh G, Agarwala S, Goh G, Dikshit V, Sing S, Yeong W (2017) Additive manufacturing in unmanned aerial vehicles (UAVs): challenges and potential. *Aerosp Sci Technol* 63:140–151
- Mohseni M, Hutmacher D, Castro N (2018) Independent evaluation of medicalgrade bioresorbable filaments for fused deposition modelling/fused filament fabrication. *Polymers*. <https://doi.org/10.3390/polym10010040>
- Zhang P, Wang Z, Junru Li J, Li X, Cheng L (2020) From materials to devices using fused deposition modeling: A state-of-art review. *Nanotechnol Rev* 9(1):1594–1609
- Mogan J, Harun W, K. K., D. Ramasamy, F. Foudzi, S. A.B., T. F. and F. Ahmad. (2023) Fused deposition modelling of polymer composite: a progress. *Polymers*. <https://doi.org/10.3390/polym15010028>
- Prajapati M, Kumar A, Lin S, Jeng J (2022) Multi-material additive manufacturing with lightweight closed-cell foam-filled lattice structures for enhanced mechanical and functional properties. *Add Manuf* 54:102766
- <https://all3dp.com/2/multi-material-3d-printing-an-overview/>, [Online].
- Rijwani T, Pi R, Asnani R, Patel N (2020) Design modification for multi-material printing with fused deposition modeling. In *Recent Adv Mech Infrastruct*. https://doi.org/10.1007/978-981-32-9971-9_12
- www.ordsolutions.com/rova3d-5-extruder-3d-printer/, [Online].
- Wang Z, Wang L, Chen J (2024) Multi-material additive manufacturing via fused deposition modeling 3D printing: A systematic review on the material feeding mechanism. *Proc Inst Mech Eng E: J Process Mech Eng*. <https://doi.org/10.1177/09544089231223316>
- Lopes L, Silva A, Carneiro O (2018) Multi-material 3D printing: The relevance of materials affinity on the Boundary Interface Performance. *Add Manuf* 23:45–52
- Baca D, Ahmad R (2020) The impact on the mechanical properties of multi-material polymers fabricated with a single mixing nozzle and multi-nozzle systems via fused deposition modeling. *Intl J Adv Manuf Technol* 106:4509–4520
- Khondoker M, Asad A, Sameoto D (2018) Printing with mechanically interlocked extrudates using a custom bi-extruder for fused deposition modelling. *Rapid Prototyp J* 24:921–934
- Teacher M, Velu R (2024) Additive manufacturing of functionally graded materials: a comprehensive review. *Int J Precis Eng Manuf* 25:165–197
- Bhavar V, Kattire P, Thakare S, Patil S, Singh R (2017) A review on functionally gradient materials (FGMs) and their applications. *Mat Sci Eng* 229:012021
- Loh GH, Pei E, Harrison D, Monzón M (2018) An overview of functionally graded additive manufacturing. *Add Manuf* 23:34–44
- Mora S, Nicola N, Pugno M, Misseroni D (2022) 3D printed architected lattice structures. *Mater Today*. <https://doi.org/10.1016/j.mattod.2022.05.008>
- Reichardt A, Shapiro A, Otis R, Dillon R, Borgoni JP, McEnerney B, Hosemann P, Beese MA (2021) Advances in additive manufacturing of metal-based functionally graded materials. *SAGE J* 66:1–29
- Li L, Sun Q, Bellehumeur C, Gu P (2002) Composite modeling and analysis for fabrication of FDM prototypes with locally controlled properties. *J Manuf Process* 4:129–141
- Ahn A, Lee H, Cho K (2024) 3D printing with a 3D printed digital material filament for programming functional gradients. *Nat Commun* 15:3605
- Baca D, Ahmad R (2020) The impact on the mechanical properties of multi-material polymers fabricated with a single mixing nozzle and multi-nozzle systems via fused deposition modeling. *Int J Adv Manuf Tech* 106:4509–4520
- Majko J, Handrik M, Vaško M, Sága M, Kopas P, Dorčiak F, Sapietová A (2023) Influence of a Directional Dependence on Mechanical Properties of Composites Reinforced with Chopped Carbon Fibre Produced by Additive Manufacturing. *Arch Metall Mater* 68(2):455–461
- T. Haruki, P. Punpongsanon and J. Kim. 2020. "Programmable filament: Printed filaments for multi-material 3D printing.,". In *the 33rd Annual ACM Symposium on User Interface Software and Technology Virtual Event USA*.

Publisher's Note Springer Nature remains neutral with regard to jurisdictional claims in published maps and institutional affiliations.